Novel insights in thrombosis pathophysiology using Mice with Impaired anticoagulation

Heestermans, M.

4

Coagulation Factor XII Does Not Contribute to Mouse Venous Thrombosis Induced By Silencing of Antithrombin and Protein C

Marco Heestermans
Tom Streef
Sander van Tilburg
Katrin Nickel
René van Oerle
Henri MH Spronk
Pieter H Reitsma
Tobias A Fuchs
Henri H Versteeg
Thomas Renné
Bart JM van Vlijmen

Manuscript under revision

Coagulation factor XII (FXII) has been proposed as a safe therapeutic drug target for venous and arterial thrombosis. Numerous experimental animal studies showed that inhibition of FXII interferes with thrombus formation, without affecting normal hemostasis (1-4). Conversely, we recently reported that inhibition of FXII by means of RNA interference (RNAi) does not confer protection in experimental VT but even augmented vascular occlusions. In a mouse model where VT follows spontaneously shortly (2-3 days) after reduction of natural anticoagulants antithrombin and protein C by RNAi (using synthetic lipid complexed siRNAs i.e. si*Serpinc1*/si*Proc*, see (5)), additional silencing of FXII (si*F12*) resulted in VT to occur even faster with a more severe thrombotic coagulopathy (figure 1A and (6)).

To dig deeper into the conflicting and unexpected finding observed upon silencing of FXII in our RNAi-based model, mice deficient for FXII (*F12*$^{-/-}$, see (2)) were subjected to the si*Serpinc1*/si*Proc* induced spontaneous VT model. Onset and incidence of the clinical phenotype that coincide with the spontaneous VT phenotype were similar in wild type (WT) and *F12*$^{-/-}$ mice (number of mice affected: WT: 9/11, *F12*$^{-/-}$: 9/11, *P*=1.0, figure 1B and figure S1A; Body weight loss: WT: -13.3% (-18.6;-8.7), *F12*$^{-/-}$: -11.7% (-15.8;-5.1), *P*=0.15, figure 1B). In addition, thrombotic coagulopathy and thrombi similarly formed in the large veins in the mandibular area of the head in WT and *F12*$^{-/-}$ mice (figure S1B and C). These observations indicate that genomic deletion of FXII (*F12*$^{-/-}$), like inhibition of *F12* by siRNA, does not confer protection in the mouse spontaneous VT model.

To clarify why siRNA-mediated *F12* silencing, in contrast to full *F12* genomic deficiency, accelerated and exacerbated the spontaneous thrombotic coagulopathy, normal female C57Black/6J mice were treated solely with siRNA against *F12* (the same si*F12* as used in (6), targeting exon 3 of the *F12* mRNA; here, si*F12*-A). As expected, si*F12*-A injected mice (without si*Serpinc1*/si*Proc* treatment) showed strong inhibition of hepatic *F12* transcript (compared to negative control siRNA i.e. siNEG injected mice; si*F12*-A: 11.3% (8.0-20.7), *P*<0.001, figure 1C). Surprisingly, plasma coagulation analysis revealed that for tissue factor (TF)-induced thrombin generation (TG) the peak height for si*F12*-A injected mice was significantly increased, compared to siNEG (siNEG; 68.9nM (65.9;74.7) and si*F12*-A: 86.8nM (82.3;95.0), *P*<0.001, figure 1D and S2A). This observation was reproduced in multiple independent experiments, with an increase of TF-induced TG peak height of approximately 20%, although it has been reported that TF-induced TG is independent on FXII activity (2).

The si*F12*-A related increase in TF-induced TG peak height was not observed for *F12*$^{-/-}$ mice, compared to WT controls (WT: 68.1nM (43.3;76.2) and *F12*$^{-/-}$: 63.3nM (62.0;66.7), *P*=0.08, figure 1D and S2A). As expected, ellagic acid (EA)-induced TG was clearly defective of plasma from *F12*$^{-/-}$ mice (figure 1E and S2B), while EA-induced TG of plasma from si*F12*-A mice was not altered despite FXII was reduced to 11% (figure 1C). Hence, the differential response for si*F12*-A treatment

and genetic *F12* deficiency in the spontaneous VT model (figure 1A and 1B) is paralleled by a differential response in plasma thrombin generation (Figure 1D and 1E), with si*F12*-A displaying an unexpected prothrombotic shift in both TG assays.

To exclude that the si*F12*-A related impact on TG is the result of si*F12*-A effects other than FXII-lowering i.e. off-target FXII-independent effects of the siRNA, two additional control siRNAs were designed. We obtained an siRNA similar to si*F12*-A, except for nucleotides 9-11 of the siRNA seed sequence which are replaced with their complementary base pairs: si*F12*-A$^{C9/11}$ (table S1). For the si*F12*-A$^{C9/11}$ mismatch control, false-positive si*F12*-A off-target effects will likely maintain their activity, whereas true positive si*F12*-A on-target effects will lose impact[7]. Moreover, an additional siRNA targeting *F12* mRNA was obtained (here, si*F12*-B), which targets exon 9 of the *F12* mRNA and inhibits *F12* mRNA more potent than si*F12*-A (figure S3). Both siRNAs were designed not to target other mRNA transcripts, which was confirmed by BLAST.

Next, mice were treated with siNEG, si*F12*-A, si*F12*-A$^{C9/11}$, or si*F12*-B (1:2 diluted with siNEG to match si*F12*-A inhibition of *F12*), and sacrificed after 3 days. Liver transcript analysis confirmed that si*F12*-A and (diluted) si*F12*-B treated mice had equal and strongly reduced *F12* hepatic transcript levels, while for control si*F12*-A$^{C9/11}$ injected mice *F12* transcript was not affected (compared to siNEG, si*F12*-A: 10.8% (3.9;19.2), si*F12*-A$^{C9/11}$: 132.8% (58.1;208.4), si*F12*-B: 10.0% (5.5;16.6), *P*<0.001, figure 1F). Remarkably, plasma from both si*F12*-A and si*F12*-A$^{C9/11}$ injected mice showed the typical prothrombotic shift in TG peak height upon TF activation (siNEG: 52.0nM (37.9;62.4), si*F12*-A: 63.3nM (51.1;74.0), si*F12*-A$^{C9/11}$: 61.0nM (47.3;68.8), *P*=0.012), figure 1G and S2C). Plasma from si*F12*-A$^{C9/11}$ injected animals responded aberrant when TG was initiated by EA, while despite low levels of FXII plasma from si*F12*-A treated mice was again not different from siNEG injected animals in TG peak height (siNEG: 47.5nM (31.3;68.6), si*F12*-A: 42.0nM (24.5;64.1), si*F12*-A$^{C9/11}$: 67.8nM (28.2;86.2), *P*=0.002, figure 1H and S2D). In contrast to si*F12*-A and similar to FXII-deficient plasma, si*F12*-B treatment did not influence the peak height in TF-induced plasma TG (siNEG: 52.0nM (37.9;62.4), si*F12*-B: 48.3nM (40.9;66.1), *P*=0.22, figure 1I and S2D), while EA-induced TG was strongly decreased in si*F12*-B plasma (siNEG: 47.5nM (31.3;68.6), si*F12*-B: 20.7nM (10.1;35.9), *P*<0.001, figure 1I and S2D). These results indicate that the observed prothrombotic shift in plasma TG upon si*F12*-A treatment cannot be attributed to FXII and appears a false-positive FXII-independent off-target effect.

The observed prolonged time to tail in the curves of TF-induced TG in si*F12*-A and si*F12*-A$^{C9/11}$ plasma (figure S2C) suggested that the plasma's ability to inhibit thrombin is affected by these siRNAs. In line with this, antithrombin levels were decreased for si*F12*-A and si*F12*-A$^{C9/11}$ mice only (compared to siNEG, si*F12*-A: 70.7% (21.7;85.4), si*F12*-A$^{C9/11}$: 74.4% (61.1;85.1), si*F12*-B: 101.9% (87.2;118.3), *P*<0.001, figure S4). Of note, in these mice a selection of liver-produced plasma

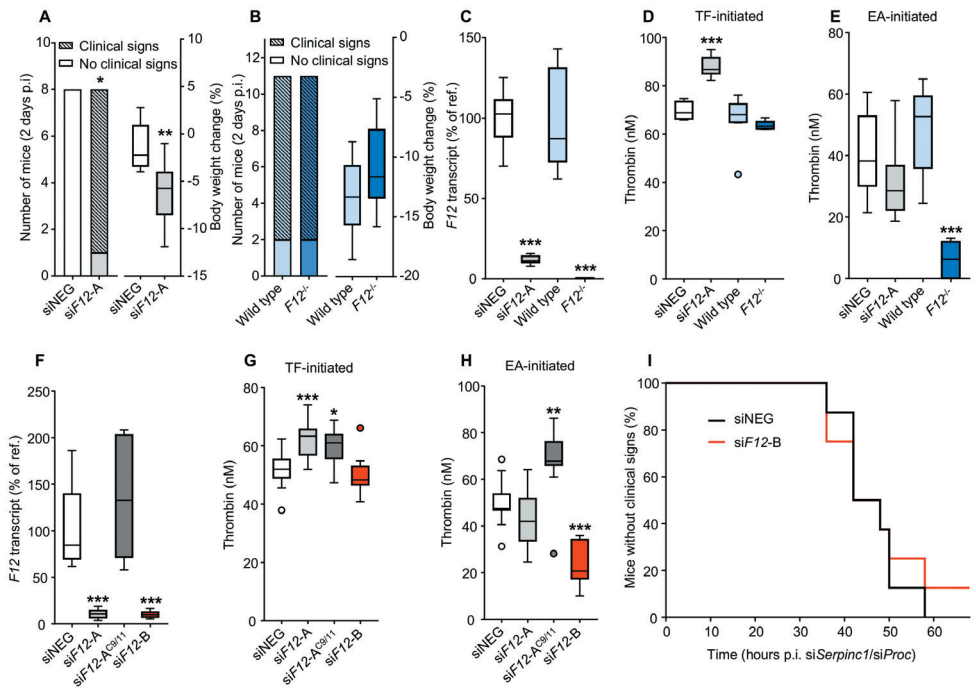

Figure 1 | Spontaneous venous thrombosis and plasma thrombin generation following silencing or deletion of factor XII. (A) Upon silencing of antithrombin and protein C (si*Serpinc1*/si*Proc* (si*Serpinc1*: cat. #S62673, si*Proc*: cat. #S72192; Ambion, Thermo Scientific, Carlsbad (CA), USA) 5.75 mg/siRNA/mouse, hepatocyte-delivered, using invivofectamine® 2.0 reagent (Thermo Scientific)), pretreatment of female C57Black/6J mice with si*F12*-A (5.75 mg siRNA/mouse, n=8, gray bars) resulted in earlier onset of spontaneous venous thrombosis, as compared to siNEG treatment (5.75 mg siRNA/mouse, n=8, white bars). This was represented as scoring of the clinical signs (left), and loss in body weight (right) 48 hours after si*Serpinc1*/si*Proc* injection (for complete methodology, see 6) (B). Upon silencing of antithrombin and protein C (si*Serpinc1*/si*Proc*, 5.75mg/siRNA/mouse), deficiency for FXII (female *F12*$^{-/-}$ mice, n=11, dark blue bars) did not affect onset (and severity, supplemental figure 2) of spontaneous venous thrombosis, as compared to wild type female C57Black/6J mice. (n=11, light blue bars). Both groups of mice had a similar (onset of) presentation of the clinical signs (left) and loss in body weight (right) 48 hours after si*Serpinc1*/si*Proc* injection (invivofectamine® 2.0 reagent, 5.75 mg/siRNA/mouse). As determined after sacrifice, silencing of hepatic *Serpinc1* and *Proc* was similar for wild type and *F12*$^{-/-}$ mice (*Serpinc1* transcript (normalized for wild type): *F12*$^{-/-}$ (median (range)): 1.13 (0.34;3.08), *P*=0.66, *Proc* transcript: *F12*$^{-/-}$: 0.90 (0.53;2.15), *P*=0.07). (C) C57Black/6J female mice were treated solely with siNEG (invivofectamine® 3.0 reagent, 1.2 mg siRNA/mouse, n=11, white bar) or si*F12*-A (1.2 mg siRNA/mouse, n=11, gray blue), or untreated and wild type (n=11, light blue bar) or deficient for *F12* (*F12*$^{-/-}$, n=12, dark blue bar). Subsequently, hepatic *F12* transcript was determined (forward primer: AATCCGTGCCTTAATGGGGG, reverse primer: TCATAGCAGGTCGCCCAAAG) with *Actb* as a house keeping gene8. (D) Plasma thrombin generation analysis was performed and thrombin peak heights determined (for thrombin generation curves, see supplemental figure 2A). Thrombin generation was initiated using 1pM tissue factor (final concentration) in 1:3 diluted mouse plasma (for a more detailed methodology, see 9). (E) Peak heights for plasma thrombin generation, initiated using 20 µg/ml ellagic acid (final concentration, for thrombin generation curves, see supplemental figure 2B). (F) Female C57Black/6J mice were treated solely

Figure 1 | Continued

with siNEG (n=11, white bars), si*F12*-A (n=11, grey bars), si*F12*-A$^{C9/11}$ (n=11, dark grey bars) and si*F12*-B (n=11, red bars, diluted 2:1 with siNEG) at a final dose of 1.2 mg siRNA/mouse, invivofectamine® 3.0 reagent). Mice were sacrificed 3 days after siRNA treatment and hepatic *F12* transcript levels were determined (*Actb* as a house keeping gene). (G and H) plasma thrombin generation were determined and peak heights displayed, initiated using (G) 1pM tissue factor (for thrombin generation curves, see supplemental figure 2C) and (H) 20µg/ml ellagic acid (for thrombin generation curves, see supplemental figure 2D. (I) Female C57Black/6J mice were injected with siNEG (n=8, black line) or si*F12*-B (n=8, red line) at a dose of 1.2 mg siRNA/mouse. One day after injection, mice were injected with siRNAs targeting antithrombin and protein C ((si*Serpinc1*/si*Proc*, 0.6 mg/siRNA/mouse, using invivofectamine 3.0). Mice were monitored and scored for clinical signs characteristic to the spontaneous VT. Once affected, mice were sacrificed. Liver *F12* transcript analysis revealed that hepatic *F12* transcript levels for the si*F12*-B mice was 9.8% (7.0;22.0) of siNEG. This lowering is comparable to residual *F12* transcript as previously observed for si*F12*-A (11.5% (6.9;20.9) of siNEG, experiment from panel A). Data are displayed in Whisker-Boxplots. *: *P*<0.05, **: *P*<0.01, ***: *P*<0.001 (compared to reference), based on Kruskal-Wallis 1 ANOVA test or Mann-Whitney U test.

protein levels (FXII-related coagulation factor XI and prekallikrein; inflammation-related proteins fibrinogen, serum amyloid A, and (the absence of) several liver enzymes) were considered normal and comparable, independent of siRNA treatment (data not shown).

In a setting of spontaneous VT, we found that si*F12*-B pre-treatment of mice did not rescue or exacerbate the thrombotic response (number of mice affected: siNEG: 8/8 and si*F12*-B: 7/8, *P*=1.0, figure 1I). This confirmed that the incidence and severity of spontaneous VT is not influenced by FXII; neither upon transient inhibition by siRNA (figure 1I) nor in permanent genetic deficiency (figure 1B).

We conclude that treatment of mice with the siRNA targeting exon 3 of the *F12* mRNA (used in (6), here si*F12*-A) induces unexpected additional changes in the plasma coagulant response, which are unrelated with FXII inhibition. The use of si*F12*-A$^{C9/11}$ let us conclude that this coagulant response of si*F12*-A is likely caused by the siRNA sequence outside the seed region. Although no indications, we cannot exclude that si*F12*-A false-positive effects go beyond coagulation. For siRNA studies, we now recommend to include C9/11 mismatch control siRNA. Although siNEG use controls for the procedure, delivery vehicles, chemistry, and activation of the RISC machinery, it appears to have insufficient ability to distinguish between true and false positives. Notwithstanding the findings, the data obtained with *F12*$^{-/-}$ and si*F12*-B injected mice let us conclude that FXII, in contrast to what has been reported for several experimental thrombosis models (2-4), does not contribute to venous thrombosis that follows spontaneously upon silencing of antithrombin and protein C in mice.

REFERENCES

1 Renne, T., Schmaier, A. H., Nickel, K. F., Blomback, M. & Maas, C. In vivo roles of factor XII. *Blood* 120, 4296-4303, doi:10.1182/blood-2012-07-292094 (2012).

2 Larsson, M. *et al.* A factor XIIa inhibitory antibody provides thromboprotection in extracorporeal circulation without increasing bleeding risk. *Sci Transl Med* 6, 222ra217, doi:10.1126/scitranslmed.3006804 (2014).

3 Matafonov, A. *et al.* Factor XII inhibition reduces thrombus formation in a primate thrombosis model. *Blood* 123, 1739-1746, doi:10.1182/blood-2013-04-499111 (2014).

4 May, F. *et al.* FXIIa inhibitor rHA-Infestin-4: Safe thromboprotection in experimental venous, arterial and foreign surface-induced thrombosis. *Br J Haematol* 173, 769-778, doi:10.1111/bjh.13990 (2016).

5 Safdar, H. *et al.* Acute and severe coagulopathy in adult mice following silencing of hepatic antithrombin and protein C production. *Blood* 121, 4413-4416, doi:10.1182/blood-2012-11-465674 (2013).

6 Heestermans, M. *et al.* Role of platelets, neutrophils, and factor XII in spontaneous venous thrombosis in mice. *Blood* 127, 2630-2637, doi:10.1182/blood-2015-10-672766 (2016).

7 Buehler, E., Chen, Y. C. & Martin, S. C911: A bench-level control for sequence specific siRNA off-target effects. *PLoS One* 7, e51942, doi:10.1371/journal.pone.0051942 (2012).

8 Safdar, H. *et al.* Modulation of mouse coagulation gene transcription following acute in vivo delivery of synthetic small interfering RNAs targeting HNF4alpha and C/EBPalpha. *PLoS One* 7, e38104, doi:10.1371/journal.pone.0038104 (2012).

9 Hemker, H. C. *et al.* The calibrated automated thrombogram (CAT): a universal routine test for hyper- and hypocoagulability. *Pathophysiol Haemost Thromb* 32, 249-253, doi:10.1159/000073575 (2002).

Supplemental table 1: siRNA sequences of si*F12*-A, si*F12*-A$^{C9/11}$, and si*F12*-B. Silencer® select siRNAs were purchased at Thermo Scientific (Waltham (MA), USA). An *in vitro* screen in mouse primary hepatocytes showed that si*F12*-A and si*F12*-B were both capable of lowering *F12* transcript equally (data not shown). Capital letters indicate complementary base pairs of the siRNA, while low case letters indicate the 3' overhang of the siRNA. For the sense-strand, two thymines are added. The seed region of all siRNA sequences are in bold. For the antisense strand, the two base pairs added are complementary with the target mRNA. The sequence of siNEG (catalog number 4390844) is not available.

siRNA	siRNA ID	Sense (5'-3')	Antisense (5'-3')
si*F12*-A	s81735	CCACAAAU**GCA**UCCACAAAtt	UUUGUGGAU**GCA**UUUGUGGtg
si*F12*-A$^{C9/11}$	s535456	CCACAAAU**CGU**UCCACAAAtt	UUUGUGGAA**CGA**UUUGUGGtg
si*F12*-B	s81736	CACCUCUA**GUU**GUCCCUGAtt	UCAGGGACA**ACU**AGAGGUGca

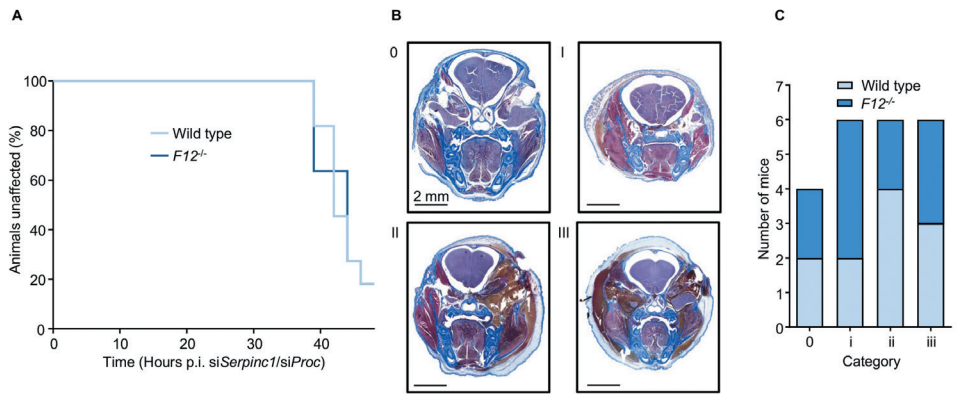

Supplemental figure 1 | Spontaneous VT progression is similar in wild type and *F12*$^{-/-}$ mice. (A) Female wild type (n=11) or *F12*$^{-/-}$ (n=11) mice were treated with siRNAs against antithrombin and protein C (si*Serpinc1*/si*Proc*, 5.75 mg/siRNA/mouse, invivofectamine® 2.0 reagent). From siRNA injection (t=0 hours), mice were inspected regularly for the presence of clinical signs of spontaneous VT. (B and C) Upon sacrifice and dissection, all mouse heads were formalin, fixed, decalcified, and embedded in paraffin. Coronal sections were made, similar as described in (6). Sections of all mice were stained using the Carstairs' methodology, and based on their thrombotic coagulopathy, severity of the phenotype was scored and subdivided in four categories (panel B): 0: no thrombotic coagulopathy, I: thrombotic coagulopathy in large veins, but no clear signs of vein rupture. Limited edema and/or bleeding, II: unilateral, thrombotic coagulopathy is clearly visible, with large thrombi associated with ruptured veins. Clear signs of edema and bleedings, III: Bilateral thrombotic coagulopathy, accompanied by edema and bleedings. (C) No significant differences in severity scores were found for the wild type and the *F12*$^{-/-}$ groups. Black bars represent 2 mm. Moreover, thrombi were scored based on structure and organization, but no differences were found. Edema, which is typical to the spontaneous VT phenotype, was quantified (measured by the thickness of the edemic dermis in coronal sections of the head, similar to (6)), but no significant differences were found. In addition, sections of mouse heads were stained for fibrin, but no differences in thrombus fibrin were observed.

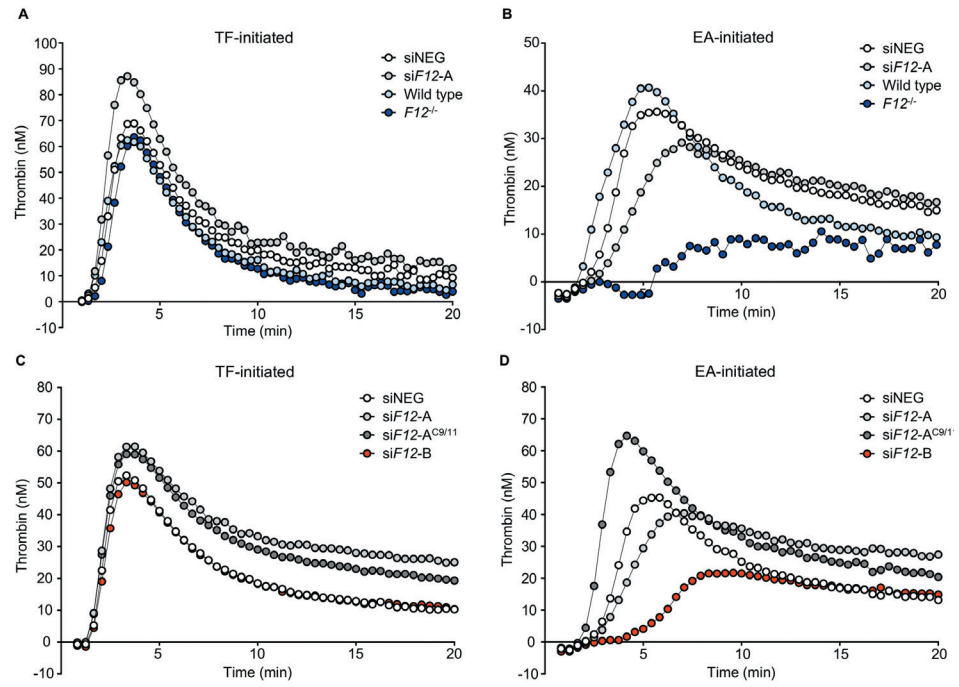

Supplemental figure 2 | Plasma thrombin generation curves of mice treated with siRNA. (A and B) Plasma thrombin generation was induced with tissue factor (end concentration of 1pM, panel A and C) or ellagic acid (20µg/ml, panel B and D). Panel A: siNEG (n=11), si*F12*-A (n=11), wild type (n=8), and *F12*$^{-/-}$ (n=6). Panel B: siNEG (n=11), si*F12*-A (n=11), wild type (n=8) *F12*$^{-/-}$ (n=8). Plasma from siNEG and si*F12*-A treated mice were collected at a different time point than plasmas from wild type and *F12*$^{-/-}$ mice. (C and D) Plasma thrombin generation was induced with tissue factor (end concentration of 1pM, panel C) or ellagic acid (20µg/ml, panel D). Panel C and D: all groups, n=11. Values below 0 are the result of an apparent incorrect calibration of the thrombinoscope, but were included in the measurement.

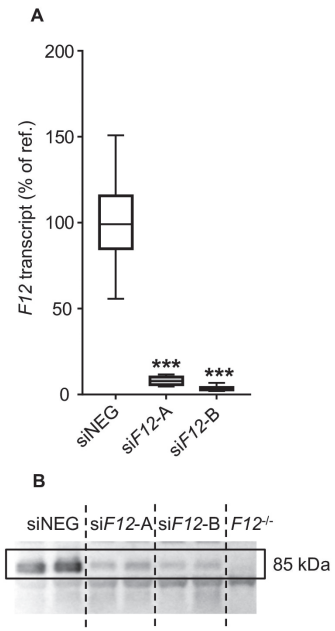

Supplemental figure 3 | si*F12*-B is more potent than si*F12*-A in inhibiting *F12* liver transcript and FXII plasma protein. (A) *F12* liver transcript upon treatment with siNEG, si*F12*-A, or si*F12*-B (all, n=8). *F12* levels were corrected for the mean of the reference group (siNEG). Data are displayed in Whisker-Boxplots. ***: *P*<0.001 (compared to siNEG), based on Mann-Whitney U-test. (B) Western Blot for FXII of representative mouse plasma samples, treated with siNEG, si*F12*-A, and si*F12*-B. The black lined square highlights the 85kDa band representing the FXII protein. FXII was detected with the 3F7 antibody. As a negative control, *F12*$^{-/-}$ mouse plasma was included.

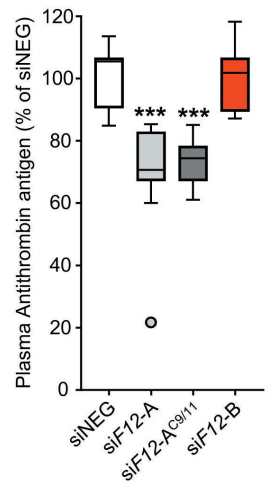

Supplemental figure 4 | si*F12*-A and si*F12*-A$^{C9/11}$ treated mice display decreased levels of plasma antithrombin. Antithrombin plasma levels were detected using the Antithrombin III murine ELISA kit (Stago, Leiden, The Netherlands). Antithrombin antigen levels were corrected for the mean of the reference group (siNEG). Data are displayed in Whisker-Boxplots. ***: *P*<0.001 (compared to siNEG), based on Mann-Whitney U-test.